ADVANCED FUNCTIONAL MATERIALS
www.afm-journal.de

A Critical Revision of the Nano-Morphology of Proton Conducting Ionomers and Polyelectrolytes for Fuel Cell Applications

Klaus-Dieter Kreuer and Giuseppe Portale*

A few aspects of the nano-morphology of hydrated Nafion and other ionomers and polyelectrolytes in their acid form are revisited by examining the evolution of small angle X-ray scattering (SAXS) data which are recorded for a wide range of water volume fractions ($\Phi_{water} \approx 7$–56 vol%). A consistency check with the recent "parallel cylinder model" discloses that this is most likely biased by a large uncertainty of the experimentally determined water content. We rather find our data to be consistent with locally flat and narrow (around 1 nm) water domains. The formation of relatively thin water "films" is suggested to be a common feature of many ionomers and polyelectrolytes, and the underlying driving force is most likely electrostatics within these highly dissociated systems. The water films may act as a charged (e.g., with positive protonic charge carriers) "glue", keeping together the oppositely charged polymer structures. While this interaction tends to produce flat morphologies, the formation process is suggested to be constraint by limited conformational degrees of freedom of the corresponding polymer and the interactions between polymer backbones. This may leave severe tortuosities on larger scales which depend on the sample history (including swelling, de-swelling, aging, stretching, and pressing).

1. Introduction

A couple of years ago, an article on the microstructure of Nafion fuel-cell membranes attracted a lot of attention, as it still does today.[1] The suggested "parallel cylinder water nanochannel" morphology seemed to naturally explain the high diffusion coefficient of water and protonic charge carriers especially at low degrees of hydration which is a common feature of perfluoro-sulfonic-acid (PFSA) membranes. This characteristic property is one of the reasons why PFSA membranes are still preferred over hydrocarbon membranes when it comes to chosing a suitable separator material for polymer electrolyte membrane (PEM) fuel-cell applications. The microstructural differences of different families of membranes and how they affect transport properties had already been described in a semi-quantitative fashion before,[2,3] but it was the work of Schmidt-Rohr and Chen that seemingly obtained the first quantitative picture of Nafion's microstructure from simulating a previously published small-angle X-ray scattering (SAXS) pattern[4] with a newly developed algorithm. This algorithm was an interesting step forward in the field and the new microstructural model of Nafion is now widely accepted and apparently supported by a recent NMR study on elongated membranes.[5] The key feature of this microstructure is inverted micelle cylinders with an average diameter of 2.4 nm for a water content as low as 20 vol%. This diameter is very large compared to the range of about 1–1.5 nm suggested before for the widths of the water structures in Nafion, implying locally more bulk like properties of the water of hydration even at very low water contents.[3] If this were true, the parallel cylinder model would dramatically change our current understanding of water and proton transport in PFSA ionomers: the transition from diffusional to hydrodynamic transport would then be expected to take place at a much lower water content, raising severe questions about the nature of water permeation and electroosmotic water drag in such structures (both are considered to have contributions from hydrodynamic transport[3]).

We have therefore revisited the structure of Nafion in its acid and Li^+ forms using data accumulated over the years supplemented by a comprehensive set of new SAXS data recorded for a large range of hydration levels. The present work comprises a consistency check of the parallel cylinder model with these data and critical remarks on what can be learned from a few SAXS patterns only. After this discussion, we present a more cautious approach taking into account that even for identifying general microstuctural features, such as the dimensionality and extension of the aqueous and polymer domains, a broad data base is needed, indeed.

But even general insights are useful for understanding the properties of PFSA membranes. They may form the basis for properties optimization with respect to PEM fuel-cell applications and provide a rationale for better understanding those common properties of ionomers and polyelectrolytes which are relevant to other established and emerging technologies. These are electrochemical

K. D. Kreuer
Max-Planck-Institut für Festkörperforschung
Heisenbergstraße 1, D-70569 Stuttgart, Germany
E-mail: kreuer@fkf.mpg.de
G. Portale
DUBBLE, BM26 at ESRF, 6 rue Jules Horowitz, BP220
F-38043 Grenoble, France

DOI: 10.1002/adfm.201300376

(e.g., redox-flow batteries, electrochemical reactors, and electrodialysis devices) and chemical applications in which the selectivity of such membranes is exploited (desalination, alcohol/water separation, etc.). Apart from the chemical nature of the membranes used for these purposes, it always comes down to their microstructure controlling the membrane properties.

2. Simulation of SAXS Patterns

2.1. Parallel Cylindrical Water Channel Model with Liquid-Like Order

According to the model introduced by Schmidt-Rohr and Chen,[1] the SAXS profile for Nafion can be reproduced by using a morphology consisting of parallel water cylinders in a polymer matrix with random packing.

An analytical description for such a system is derived here. According to the decoupling approximation, the scattered intensity can be written as:

$$I(q) = C\left\langle F(q)^2\right\rangle\left[1 + \beta(q)\left(S(q) - 1\right)\right]$$

where $F(q)$ is the scattering amplitude of the cylindrical domains and $S(q)$ the lattice factor. C is a constant proportional to the square of the electron density difference between water and polymer matrix, to the cylinder volume and to the number of cylinders.

The term $\beta(q)$ is given by:

$$\beta(q) = \frac{\left\langle F(q)\right\rangle^2}{\left\langle F^2(q)\right\rangle}$$

The scattered amplitude for any object is given by the Fourier transform of its electron density distribution $\rho(\vec{r})$. In the case ρ is constant inside the object, the scattering amplitude is written as:

$$F(\vec{q}) = \rho \int_V \exp(i\,\vec{q}\,\vec{r})\,d\vec{r}$$

For a homogeneous cylinder of length L and radius R, this is conveniently expressed in cylindrical coordinates:

$$F(\vec{q}) = \rho \int_{-L/2}^{L/2}\int_0^R\int_0^{2\pi} \exp(-i\,\vec{q}\,\vec{r})\,r'\,d\phi\,dr'\,dz$$

where r' φ and z are the coordinates within a reference system with the axis z being identical with the cylinder axes. The scattering vector $\vec{q} = (q_x, q_y, q_z)$ is expressed in cylindrical coordinates according to:

$$q_x = q(\cos\alpha\,\cos\gamma\,\cos\theta + \sin\gamma\,\sin\theta)$$

$$q_y = -\,q\,\sin\alpha\cos\theta$$

$$q_z = q\,(\cos\alpha\sin\gamma\cos\theta - \cos\gamma\sin\theta)$$

where θ is half of the scattering angle, α is the azimuthal angle in the detector plane, and the detector and γ is the angle between the X-ray beam and the cylinder axis.

The scattered amplitude can be further reduced to:[6]

$$F(q,\gamma) = \frac{\sin(q\,L\sin\gamma/2)}{(q\,L\sin\gamma/2)}\left(2\frac{J_1(q\,R\cos\gamma)}{(q\,R\cos\gamma)}\right)$$

where $J_1(x)$ is the cylindrical Bessel function of the first order:

$$J_1(x) = \frac{1}{2\pi}\int_{-\pi}^{\pi} e^{-i(\tau - x\sin(\tau))}\,d\tau$$

In this way, the scattering amplitude is calculated for any angle γ, i.e. for any cylinder orientation with respect to the beam. In the case of random orientation of the cylinders, the total intensity is calculated as:

$$I(q) = \int_0^{\pi/2}\left\langle F(q,\gamma)^2\right\rangle\sin\gamma\,d\gamma$$

While there is no analytical solution for the structure factor of short cylinders packed with no preferential orientation available yet, the limiting case of very long parallel cylinders is easier to handle. In this case, the system can be defined just by the cylinder packing in the plane perpendicular to the cylinder axis. Such arrangements are reminiscent to these of hard discs interacting only in the disk plane direction, and the structure factor proposed by Rosenfeld can be used:[7]

$$\frac{1}{\mathrm{S(q)}} - 1 = 4\eta\left\{A\left[\frac{J_1(q\,R)}{q\,R}\right]^2 + BJ_0(q\,R)\frac{J_1(q\,R)}{q\,R} + G\frac{J_1(2q\,R_{HD})}{q\,R}\right\}$$

where R_{HD} is the separation of neighboring hard discs, and

$$A = \left[1 + (2\eta - 1)\chi + 2\eta G\right]/\eta$$

$$B = \left[(1-\eta)\chi - 1 - 3\eta G\right]/\eta$$

$$\chi = (1-\eta)/(1-\eta)^3$$

$$G = 1/(1-\eta)^{3/2}$$

Such a structure factor shows a first order peak at a q value determined by the radius of the cylinders and their average distance. Its intensity is dominated by the "hard-disk" volume fraction η.

For long parallel cylinder arrangements the volume fraction η of the hard-disc model translates into the water volume fraction Φ_{water} in the following way:

$$\Phi_{\mathrm{water}} = \eta\Big/\left(\frac{R_{\mathrm{HD}}}{R_{\mathrm{W}}}\right)^2$$

with R_W being the cylinder radius.

In the present work, we have refined Φ_{W} by either varying η and keeping $R_{\mathrm{HD}}/R_{\mathrm{W}}$ fixed or vice versa.

2.2. Film-Like Morphology Model Using Paracrystalline Theory

For stacks of alternating flat water and polymer objects with lateral extensions significantly larger than the object thicknesses,

the position of the ionomer peak (scattering peak typical for phase separated ionomers) is given by the structural correlation length d along the stacking direction ($d = d_p + d_w$ where p and w stand for polymer layer and water layer respectively). Structural disorder introduced as variations in the water domain separation distance determines the width of the ionomer peak.[8,9]

The intensity scattered by such a system as a function of the scattering vector q is then:

$$\frac{d\sigma}{d\Omega}(q) = \left[\int_0^\infty D(x)\,F^2(q,x)dx\right] S(q)$$

with $F^2(q, x)$ being the square of the layer scattering amplitude, i.e. the form factor of a homogeneous layer of thickness x:

$$F^2(q, x) \propto \left[\sin(qx/2)/(qx/2)\right]^2$$

and $D(x)$ being the thickness distribution function of the water layers.

$S(q)$ is the structure factor for a multi-layered system with paracrystalline disorder which is written as:[10]

$$S(q,N,d,\Delta,N_{diff}) = N_{diff} + \sum_{N_k=N-2\sigma}^{N+2\sigma} x_k\left(N_k + 2\sum_{m=1}^{N_k-1}(N_k-m)\cos(mqd)\exp\left(-\frac{m^2q^2\Delta^2}{2}\right)\right)$$

where the vector $q = q_z$ is in the direction perpendicular to the lamellar plane. The mean square fluctuation of the distance between water layers Δ is introduced as to describe the stacking disorder of the system. N_{diff} accounts for an additional diffuse background originating from uncorrelated water layers. The strong attenuation of the structure factor oscillations with increasing q_z is taken into account by the Gaussian function x_k:

$$x_k = \frac{1}{\sigma\sqrt{2\pi}}\exp\left[-\frac{(N_k-N)2}{2\sigma^2}\right]$$

with:

$$\sigma = \begin{cases}\sqrt{N} \text{ for } N \geq 5\\ (N-1)/2 \text{ for } N < 5\end{cases}$$

where N is the mean number of stacks and N_k is one of the water layers in the range $N \pm 2\sigma$.

3. Critique of the "Parallel Cylinder Model"

Schmidt-Rohr and Chen simulated the SAXS patterns of a variety of structural models such as Gierke's historical cluster model,[11] the fibrillar (bundle) model brought up by the Grenoble group[12] and, of course, their parallel cylinder model in the q range 0.05–4 nm^{-1} testing the agreement with the corresponding part of a SAXS pattern recorded by Rubatat et al. on "swollen" Nafion in its Li$^+$-form over an even larger q range.[4] All models assume the existence of a distinct polymeric and aqueous phase without internal structure, which is justified by the choice of the q-range (corresponding to length scales > 1 nm in real space which is far beyond the molecular fine structure).

The fact that the parallel cylinder model was the only one perfectly matching the experimental SAXS pattern then seemed to provide strong evidence for this model to be close to the real nano morphology of Nafion.

In the following, we will show that this conclusion is biased by a significant error of the experimentally determined water volume fraction. Since a single high quality SAXS pattern was used for this simulation study only (some patterns with low S/R from the historical work of Gierke[11] were also included), the result of the model discrimination depended very much on the water content which was no degree of freedom in the simulation procedure. There was only some freedom in the size and concentration of crystallites, but all other parameters were constrained through the choice of the model including the water volume fraction.

For this, the authors used 20 vol%, a value given for a pattern in Figure 2 of the paper by Rubatat et al.[4] which resembles the pattern given in **Figure 1** of the same paper, however, with intensities about nine orders of magnitude lower. Since this study covers an amazingly large range of water concentrations, a precise determination of the water content for each sample was not very important; but for the simulation work of Schmidt-Rohr and Chen which relies on a single pattern, this was absolutely critical.

The position of the ionomer peak in the SAXS pattern is actually a reliable indicator for the water content. With the reasonable assumption that lithium neutralization does not

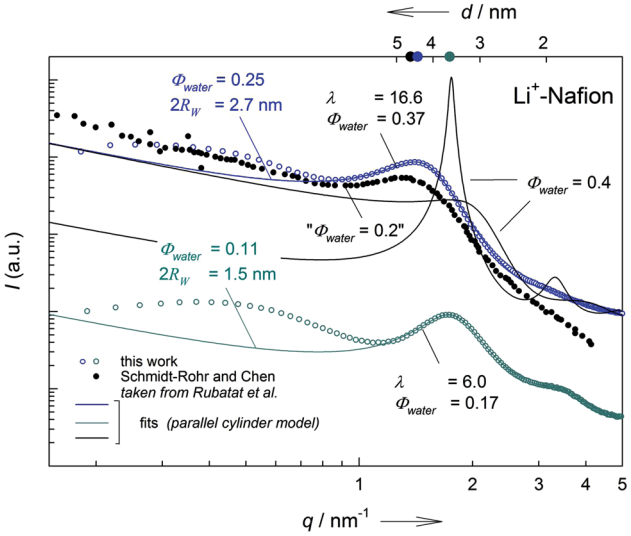

Figure 1. SAXS patterns of Li$^+$-exchanged Nafion for two different water volume fractions compared to the diffraction pattern reported by Rubatat et al.[4] and used by Schmidt-Rohr and Chen[1] for their simulation work. For reasons of clarity, the two sets of patterns are shifted on the logarithmic intensity scale with respect to each other, i.e. absolute intensities are not shown here. The characteristic correlation lengths are indicated on the upper abscissa. The two patterns of the present work are fitted with parallel water cylinder morphologies leaving the water volume fraction Φ_{water} and the cylinder diameter $2R_W$ as free parameters, the former refining to significantly lower values than the experimental ones (0.25 compared to 0.37 and 0.11 compared to 0.17). Two fits for a fixed water volume fraction of 0.40 are also included (see text).

change the morphology (in particular the correlation length) too much,[13] the position of the ionomer peak around $q = 1.4$ nm^{-1} (corresponding to $d = 4.5$ nm) suggests a water content of ≈40 vol% corresponding to $\lambda = [H_2O]/[\text{-}SO_3H] \approx 19$, which is the approximate water content after soaking in water (see also below discussion on the relation between water content and correlation length in the acid form). In order to proof the above assumption we have ion exchanged Nafion 117 into its Li^+-form and recorded the SAXS patterns in the swollen state and after equilibrated at RH = 75%, respectively corresponding to water contents of 37 and 17 vol%. Comparing shape and position of the ionomer peak of both with those of the pattern used by Schmidt-Rohr and Chen (Figure 1) clearly indicates that the water content of the latter must have been around 40 vol%, which is two times 20 vol%.

For SAXS measurements, usually small samples (some 10 mg) with absolute water contents in the mg range are used, which makes difficult a quantitative determination of the hydration number by weighing hydrated and dried samples. For the patterns discussed in the next section, we have therefore taken special care in the determination of the hydration level, and we have used a considerable number of patterns which reduces statistical errors.

Since we did not have access to the numerical code used by Schmidt-Rohr and Chen, we have used an analytical solution for the SAXS intensity $I(q)$ for water cylinders arranged in a parallel fashion within a Teflon matrix to fit the SAXS patterns, leaving the water content as a free parameter. As seen in Figure 1, very good fits were obtained, but only with water contents significantly lower than the experimental ones (25 compared to 37 vol% and 11 compared to 17 vol%), while a fixed water content of 40 vol% did not allow for any reasonable fit (neither peak position nor peak shape could be reproduced).

We have restricted the fits to a relatively small q-range because the SAXS pattern of Nafion severely changes with time and pre-treatment; i.e. there is nothing like "the" morphology of Nafion. While the high-q part ($q > 0.3$ nm^{-1}) is reasonably reproducible and only little affected, the low-q part slowly but severely changes with time (**Figure 2**). SAXS patterns of as received samples are essentially flat in this range, and it is the standardization process (treating in hot acid and rinsing with water) that leads to a steep upturn of the scattering intensity at low q. This slowly decays when the sample is kept in water with all changes being reversed after repeated standardization (Figure 2). It should be noted that the steep upturn observed after standardization is reminiscent of the ultra small angle upturn already observed by Rubatat et al. for much lower q,[4] and one may suspect that this is just shifting to lower q with time.

The q^{-1} behavior at low q therefore appears to be a special case only, but for any simulation approach, this feature reduces possible models to these with objects elongated in one direction (in the 30–100 nm range). For Rubatat et al. these were polymer fibrillar/bundles[4,12] while Schmidt-Rohr and Chen were biased towards the complementary structure containing elongated water cylinders because of the very small faulty volume fraction of water (see above).

Another important aspect, which must be mentioned, is the ambiguity of the procedure chosen by Schmidt-Rohr and Chen. This is just discrimination between more or less reasonably chosen models by examining the agreement of their simulated SAXS pattern with experimental SAXS data. With the assumption of a too small water content (20 vol%), the "parallel cylinder model" was the only one matching the experimental data, indeed. But with a water content around 40 vol%, the high q-part of the data can easily be reproduced by a variety of models: the ionomer peak essentially contains information on the structural correlation length including its distribution and the Porod-regime (q^{-4} behavior) on the extension of the internal water/polymer interface. These two features can be reproduced within the constraints of different models, which was recently also recognized by a simulation work on the same ionomer.[14] It is therefore not surprising that SAXS patterns of chemically very different ionomers are similar in this q-range.[2] In our comparative study on different types of ionomers, we had therefore decided to use only above mentioned *"hard"* parameters which can reliably be obtained from SAXS data.[2]

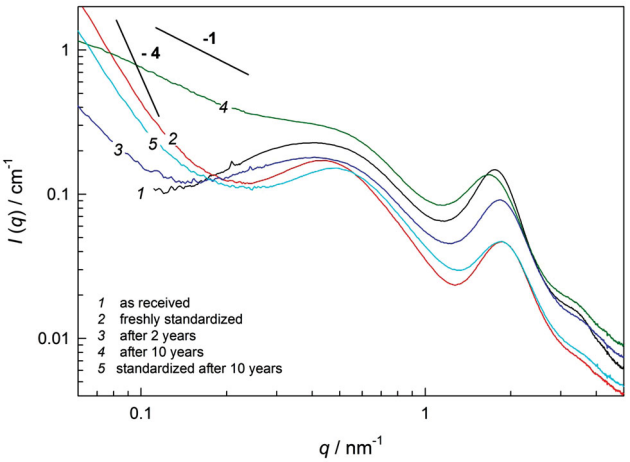

Figure 2. The evolution of H^+-Nafion SAXS patterns with time and treatment. The measurements were taken in air corresponding to a water content $\lambda \approx 4$ for all samples.

Eventually, any structural model must be in accordance with physicochemical principles. A cylindrical shape of the water structures with the negative charges at the surface (water/polymer interface) and the positive charges (acid protons) in the interior corresponds to a significant separation of charges and a severe accumulation of positive charges within the cylinders. Considering electrostatics only, any flattening of such structures is energetically more favorable as long as the separated charges are not completely screened by the high dielectric solvent (water). Indeed, for perfluorinated surfactant/water mixtures, Lyonnard et al. found a hexagonal phase which is reminiscent of "water cylinders" in Nafion at very high water contents only, while a lamella phase appeared to be stable up to a water content of ≈40 vol%.[15]

One also has to consider the adjustment of the morphology to changing water contents. For any cylindrical water structure, some rearrangement within the polymer domain is required. Assuming the number of cylinders per polymer volume being constant (as Schmidt-Rohr and Chen did), the extension of the water/polymer interface must increase and the density of

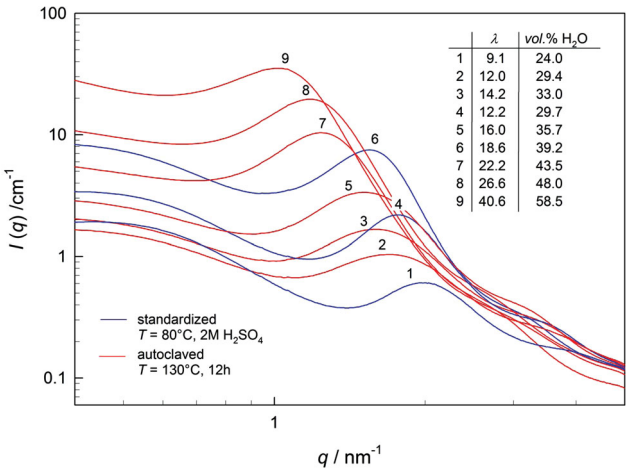

Figure 3. SAXS patterns of Nafion in its acid form for a few selected water contents. The two data sets correspond to different pre-treatments (see the Experimental Section).

negative charges at this interface must decrease with hydration, which is actually not observed as will be shown later. The only consistent way within the cylinder model allowing to increase the water content without changing the internal interface is to decrease the number of cylinders with increasing hydration which would actually lead to a strong increase of the structural correlation length with increasing hydration. Moreover, this also requires severe structural reorganization within the polymer domain with a probably sluggish response.

4. An Alternative Approach to Understand the Morphology of Nafion

In order to reduce the ambiguity of our understanding of Nafion's microstructure, we have therefore expanded the data base and basic physicochemical aspects have been included into our considerations.

SAXS patterns of Nafion in the acid form with water contents ranging from ≈25 to ≈60 vol% (**Figure 3**) were recorded within the relatively well reproducible q-range containing the ionomer peak and the Porod regime. The highest water contents could only be obtained by treating Nafion in a water-filled autoclave at $T = 130$ °C, which actually leads to some broadening (Figure 3) and small offset (**Figure 4**a) of the ionomer peak's position to lower q, which will not be discussed in this article.

The shift of the ionomer peak to lower q with increasing water content (swelling) is clearly visible, and a double logarithmic plot of the corresponding correlation length versus the polymer volume fraction $\Phi_{polymer}$ reveals a close to linear dependence (Figure 4a), while the linear plot versus the ratio of water and polymer volume fractions (Figure 4b) even shows a close to proportional behavior. The latter points towards swelling in a single direction as expected for a locally two-dimensional structure such as the "lamellar" structure suggested by Litt et al,[16] the "sandwich-like" structure proposed by Haubold et al.,[17] or the flat "ribbons" brought up by the Grenoble group.[4,12] Most of these models are based on the

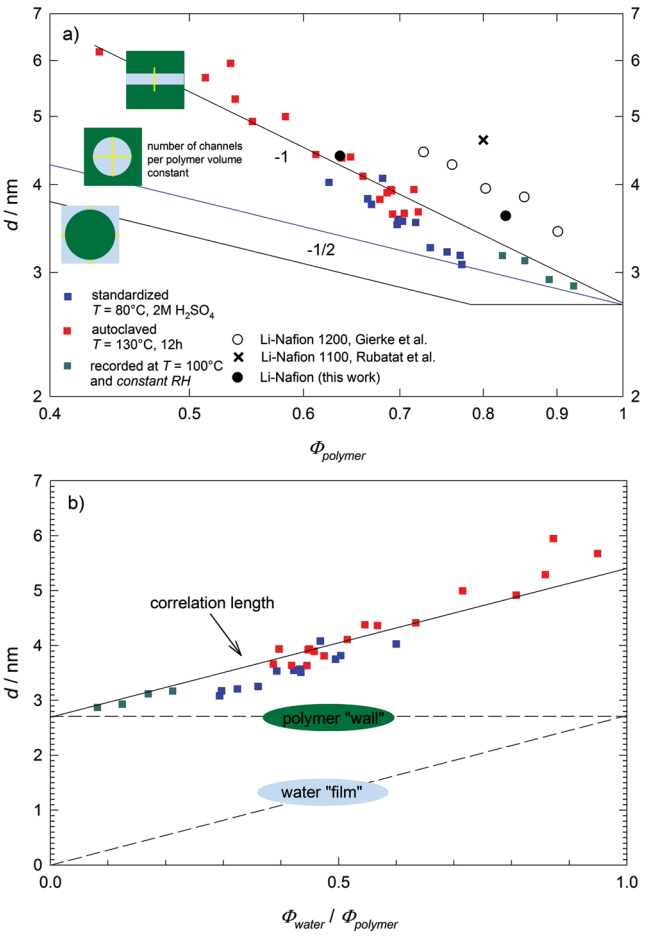

Figure 4. a) Evolution of the structural correlation length d with the degree of hydration as obtained from the position of the ionomer peak in double logarithmic representation versus the polymer volume fraction $\Phi_{polymer}$ together with the characteristics expected for three idealized situations (uniform water cylinders in polymer matrix, uniform polymer layers separated by water films, uniform polymer rods in a water matrix as schematically illustrated), data from Gierke et al.[11] and Rubatat et al.[12] are shown for comparison. b) Linear representation of the data as a function of the ratio of water and polymer volume fractions $\Phi_{water}/\Phi_{polymer}$ together with the polymer "wall" and water "film" thicknesses expected for a layered morphology. Note: the values at low water contents (light blue) are obtained at $T = 100$ °C and controlled RH (not published yet).

observation that the correlation length shows approximately linear scaling with the water volume fraction. Swelling of a constant number of cylinders (as proposed by Schmidt-Rohr and Chen) or swelling of the inverse structure (water between rod-like polymer aggregates) in two directions would result in different dependencies (Figure 4a).

Omitting any details of the shape of such a "water film", its average thickness would then increase proportionally with the water content, the thickness of the "polymer walls" remaining constant at around 2.7 nm. This interpretation of the evolution of the ionomer peak is also consistent with the analysis of the Porod-regime at higher q from which the extension of the inner water/polymer interface is obtained.[3,18] **Figure 5** shows this interface per volume (S/V) together with the corresponding data

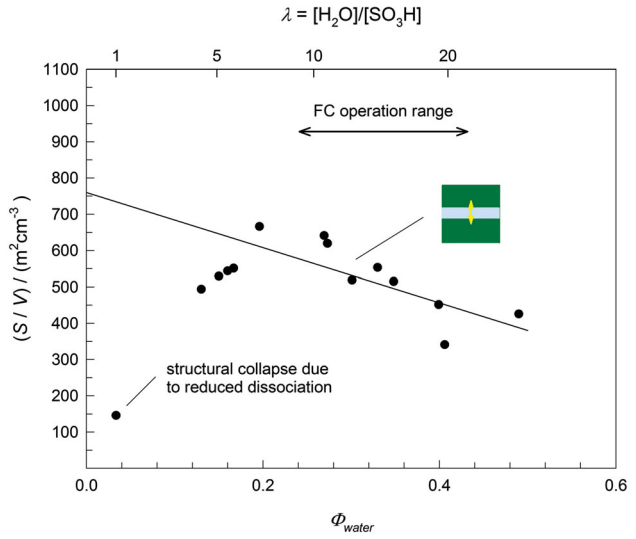

Figure 5. Internal interface to volume ratio (S/V) as obtained from the Porod regime as a function of the water volume fraction Φ_{water}.[18] For comparison, the values calculated for a layered morphology using polymer and water layer thicknesses shown in Figure 4b are shown as the line.

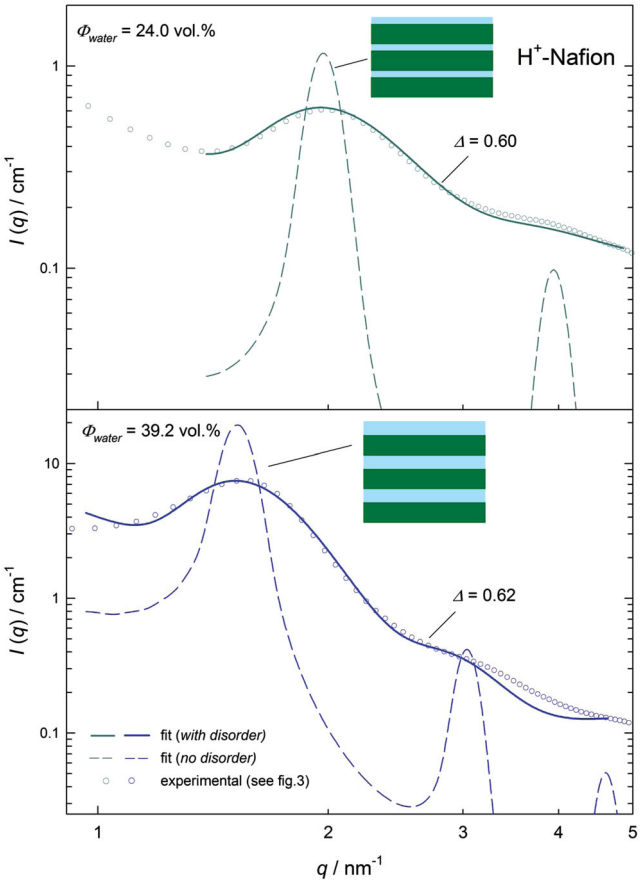

Figure 6. SAXS patterns of Nafion in its acid form for two water contents (taken from Figure 3) and best fits for paracrystalline morphologies of stacked planar polymer and water sheets. Note that, for the simulation, the water contents were fixed to the experimental ones leaving the widths of the polymer and water phases and the degree of disorder Δ as the only fit parameters.

expected for a two dimensional film morphology with polymer and water film thicknesses given in Figure 4b. The agreement is remarkable especially in the water volume range 20–50 vol% where the Porod regime extends over approximately two orders of magnitude in scattered intensity. While this makes the calculation of S/V quite reliable, the error bars significantly increase at lower water content where the Porod decay progressively loses its significance, which may explain the small deviations around 10 vol% water. The single data point around 5 vol% ($\lambda \approx 1$) is completely irrelevant to the present considerations not only because it is based on a hardly visible Porod behavior, but also because of the low dissociation of the sulfonic acid groups at such a low water content.[19] As we will explain later, the electrostatic interactions which depend on the degree of dissociation are probably driving the formation of Nafion's microstructure on the nm scale. For an almost neutral system we actually expect a collapse of the structure on this scale associated with the disappearance of the inner water/polymer interface at low water contents.

Kong and Schmidt-Rohr have recently used these data for supporting their "parallel cylinder model"[20] arguing that this is the relevant range of water volume fractions for fuel cell applications. In a running fuel cell the anode side of the membrane may dry out at high current densities as a consequence of high electroosmotic water drag,[21] and this leads to severe ohmic polarization losses which are not characteristic of normal operating conditions. In Figure 5, we have therefore also included the approximate range of water volume fractions which may occur under regular fuel cell conditions. But it should also be emphasized that especially low water contents favor flat water structures acting as electrostatic cross-links between polymer domains provided the water content is high enough to ensure a high degree of dissociation.

From above considerations it is clear that the experimental SAXS patterns must be reproduced by calculating $I(q)$ for planar objects piled to form stacks with paracrystalline order. We have done this for two SAXS patterns of Nafion in its acid form, fixing the water volume fractions Φ_{water} to the experimental ones (24 and 39.2 vol%) which leaves the degree of disorder as the only free parameter. The comparison of the experimental SAXS patterns with the simulated ones of well ordered stacks nicely shows that the structure (bumps) within the Porod regime most likely stems from higher order diffraction (**Figure 6**). By introducing some disorder, the diffraction peaks broaden and surprisingly good fits are obtained in the q range 1.5–5 nm^{-1}. For lower q, the simulated intensity increases with q^{-2} for stacks of extended sheets, and the fact that this feature is not consistently observed experimentally (Figure 2) suggests that the structures are close to planar on a local scale only ($\leq$ 4 nm) with tortuosities on longer scales depending on pretreatment and relaxation processes (see above).

5. Generalization

Finally, we would also like to mention that "film-like" water structures are consistent with other properties of Nafion and

probably apply to the microstructure of ionomers and polyelectrolytes in general. The response of Nafion to changes of the water activity (RH) in its environment is quasi instantaneous provided the membrane surface is wetted with water. This, we observe for weight changes measured in TGA experiments, responses of the viscoelastic properties seen by DMA or conductivity changes induced by alterations of the humidification conditions. The latter is demonstrated in **Figure 7** showing the conductivity of a ≈100-µm-thick PFSA membrane in ambient air sprayed with water from one side. 90% of the response takes place within ≈10 seconds which is expected for a diffusion controlled process. Recent experimental work of Kusoglu et al.[22] and Lyonnard et al.[23] provides strong evidence for an even faster structural response, which is strongly pointing towards a locally one-dimensional swelling of a "layered" water/polymer morphology.

There is actually first indication that this structural motif is quite universal. **Figure 8** shows the evolution of the correlation lengths (obtained from the position of the ionomer peak) recorded for a sulfonated poly (phenylene ether ketone) and a highly sulfonated poly (phenylene sulfone) (which is a polyelectrolyte) as a function of the polymer volume fraction. Although the correlation lengths differ a lot, they all increase in a close to linear fashion with decreasing polymer volume fraction.

The reason for this striking observation may simply be electrostatics. The charge distributions in "cylindrical" and "film-like" water structures schematically illustrated in **Figure 9** correspond to significantly different electrostatic energies: in flat structures positively charged protonic defects may stabilize between negatively charged sulfonate counter ions located on different polymer objects participating in ionic cross-links, and there is more freedom to avoid disadvantageous accumulation of positive charges than in cylindrical water structures. The electrostatic interactions mediated by water "films" may have a stabilizing effect on the morphology of ionomers and polyelectrolytes: thin water structures act as positively charged "glue" keeping together the negatively charged ionomer structures. Apart from electrostatics, there are additional interactions driving the microstructure of ionomers, but this we will

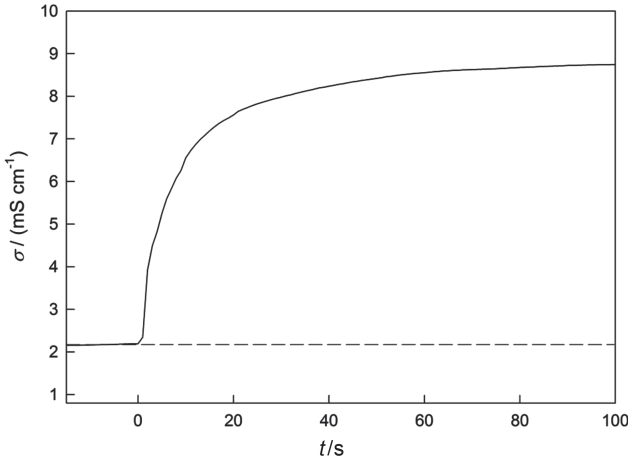

Figure 7. Conductivity response of a Nafion membrane in air after spraying water onto one membrane side.

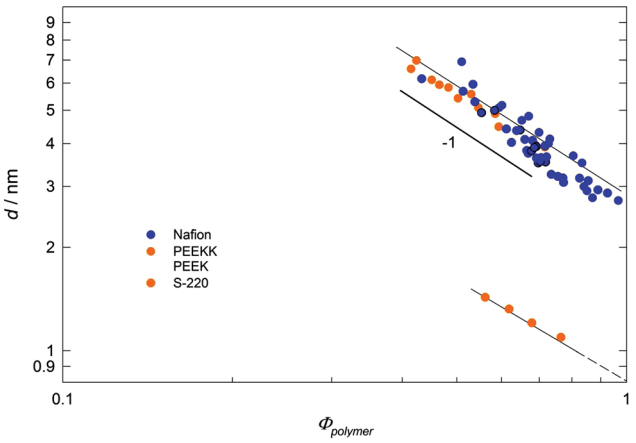

Figure 8. Structural correlation length d as a function of polymer volume fraction $\Phi_{polymer}$ for different ionomers and a polyelectrolyte[3] (S-220: fully sulfonated poly(phenylene sulfone)).[24]

discuss in a forthcoming paper on the evolution of the microstructure of ionomers and polyelectrolytes with temperature and relative humidity. We will also separately discuss the NMR work[5] apparently supporting the parallel cylinder model. One key result there is that the Nafion morphology shows tortuosities on the ≈30–100 nm scale which are strongly affected by pre-treatment and relaxation effects (see also Figure 2). But on the nanometer scale, the "film-like" morphology suggested here appears to be quite robust. Only at very high water contents (>50 vol%) a progressive buckling followed by a phase inversion as suggested by Gebel et al. is expected.[12] Of course, any nano-mophology must be consistent with the molecular structure of the ionomer and its possible conformations. In the case of Nafion, one may speculate that the average width of the polymer objects (≈2.7 nm) corresponds to the thickness of amphiphilic bilayers. Unfortunately, the understanding of this multi-scale situation is still in its infancy.

6. Morphology and Transport

The question remains in which way the microstructure of Nafion relates to its high proton conductivity at low degrees of hydration. In fact, the soft side-chain architecture shows a more developed hydrophobic/hydrophilic separation with wider aqueous domains than observed for short side chain ionomers[21] and for typical hydrocarbon membranes.[2,3,25] This together with the pronounced hydrophobicity of the backbone may lead to a higher local (few nm scale) fluidity of the aqueous phase. The lower tortuosity (on a larger scale), resulting from the larger backbone persistence length characteristic to PFSAs compared to hydrocarbons, may lead to a more efficient percolation within the proton conducting aqueous domain.

7. Experimental Section

Sample Preparation: Nafion 117 was standardized by keeping in 2M H_2SO_4 at T = 80 °C for 2 h before rinsing with water until neutrality.

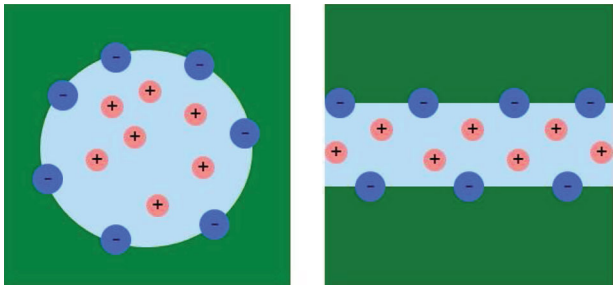

Figure 9. Schematic illustration of the distribution of ionic charges in cylindrical and flat water structures. Note that flat water structures correspond to more negative electrostatic energies.

Li^+-Nafion was obtained by exchanging the acid form two times in an excess of 1 M LiOH for one day, again before rinsing with water. Membrane slices in the acid and Li^+ forms (5 mm in diameter) were punched and two of them were stacked in a gas tight brass cell with two thin Mylar sheets serving as windows for SAXS measurements. For adjusting different water contents, the cells were kept open on a balance before closing until the targeted water content was approximately achieved. The water contents were precisely determined by weighing the hydrated membranes, the cell with the membranes in the hydrated state before and after the measurements and finally the membranes in the dry state. The membranes were dried at T = 140 °C for one day in vacuum. In this way, water contents in the range λ = 9.1–18.6 (corresponding to 24–39.2 vol%) were adjusted. For calculating the water volume fractions, 1 g cm^{-3} and 2.12 g cm^{-3} were taken as densities of the water and Nafion volume increments, respectively. For achieving higher water contents, standardized membranes were additionally treated in an autoclave filled with water and kept at T = 130 °C for one night. Again, by varying the drying period, hydration levels in the range λ = 12–40.6 (29.4–58.5 vol%) were adjusted.

Small Angle X-Ray Scattering (SAXS): SAXS experiments were performed at the DUBBLE beam line (BM 26B) of the European Synchrotron Radiation Facility (ESRF) in Grenoble (France).[26] The data were collected using a Pilatus photon counting detector with pixel array dimensions of 1043 µm × 981 µm and 172 µm × 172 µm pixel size. The exposure time for each sample was about 60 s and a wavelength of λ = 1.033 Å was applied. A sample-to-detector distance of 1.5 m was used. The q-scale ($q = 4\pi\sin\theta/\lambda_{X\text{-ray}}$, where 2θ is the scattering angle and $\lambda_{X\text{-ray}}$ is the X-ray wavelength) was calibrated using the positions of diffraction peaks of a standard silver behenate powder. The absolute intensity was calibrated using two secondary intensity standards, i.e., water and Lupolen. The experimental data were corrected for background scattering and transformed into 1D plots by azimuthal angle integration before calibration in absolute intensity. SAXS patterns of aged samples were recorded in a similar way on the beam line CRG D2AM of ESRF as well.

Acknowledgements

We thank R. Dinnebier (Max-Planck-Institut für Festkörperforschung) for reading the poofs; S. Lyonnard (CEA, Grenoble) for recording the SAXS patterns shown in Figure 2, K. Schmidt-Rohr (Iowa State University, Ames), G. Gebel and O. Diat (CEA, Grenoble) for sharing their thoughts with us, and A. Fuchs and U. Klock for technical assistance.

Received: January 30, 2013
Revised: April 14, 2013
Published online: June 3, 2013

[1] K. Schmidt-Rohr, Q. Chen, *Nat. Mater.* **2008**, *7*, 75.
[2] K. D. Kreuer, *J. Membr. Sci.* **2001**, *185*, 29.
[3] K. D. Kreuer, S. J. Paddison, E. Spohr, M. Schuster, *Chem. Rev.* **2004**, *104*, 4637.
[4] L. Rubatat, A. L. Rollet, G. Gebel, O. Diat, *Macromolecules* **2002**, *35*, 4050.
[5] J. Li, J. K. Park, R. B. Moore, L. A. Madsen, *Nat. Mater.* **2011**, *10*, 507.
[6] G. Porod: *Small-Angle X-ray Scattering* (Eds. O. Glatter, O. Kratky), Academic Press, London **1982**, pp. 119–196.
[7] Y. Rosenfeld, *Phys. Rev. A* **1990**, *42*, 5978.
[8] R. Hosemann, S.N. Bagchi, *Direct Analysis of Diffraction by Matter*, North-Holland, Amsterdam **1962**.
[9] R. Bonart, R. Hosemann, *Kolloid Z. Z. Polym.* **1962**, *186*, 16.
[10] T. Frühwirth, G. Fritz, N. Freiberger, O. Glatter, *J. Appl. Crystallogr.* **2004**, *37*, 703.
[11] T. D. Gierke, G. E. Munn, F. C. Wilson, *J. Polym. Sci. B: Polym. Phys.* **1981**, *19*, 1687.
[12] L. Rubatat, G. Gebel, O. Diat, *Macromolecules* **2004**, *37*, 7772.
[13] A. L. Rollet, G. Gebel, J. P. Simonin, P. Turq, *J. Polym. Sci. B: Polym. Phys.* **2001**, *39*, 548.
[14] C. K. Knox, G. A. Voth, *J. Phys. Chem. B* **2010**, *114*, 3205.
[15] S. Lyonnard, Q. Berrod, B. A. Grüning, G. Gebel, A. Guillermo, H. Ftouni, J. Ollivier, B. Frick, *Eur. Phys. J.: Spec. Top.* **2010**, *198*, 205.
[16] M. H. Litt, *Polym. Prepr.* **1997**, *38*, 80.
[17] H. G. Haubold, T. Vad, H. Jungbluth, P. Hiller, *Electrochim. Acta* **2001**, *46*, 1559.
[18] M. Ise, PhD Thesis, University of Stuttgart, Germany **2000**.
[19] A. Telfah, G. Majer, K. D. Kreuer, M. Schuster, J. Maier, *Solid State Ionics* **2010**, *181*, 461.
[20] X. Kong, K. Schmidt-Rohr, *Polymer* **2011**, *52*, 1971.
[21] K. D. Kreuer, M. Schuster, B. Obliers, O. Diat, U. Traub, A. Fuchs, U. Klock, S. J. Paddison, J. Maier, *J. Power Sources* **2008**, *178*, 499.
[22] A. Kusoglu, M. A. Modestino, A. Hexemer, R. A. Segalman, A. Z. Weber, *ACS Macro Lett.* **2012**, *1*, 33.
[23] S. Lyonnard, Q. Berrod, G. Gebel, A. Guillermo, *E-MRS Spring Meeting, Symposium F*, Strasbourg **2012**.
[24] C. C. de Araujo, K. D. Kreuer, M. Schuster, G. Portale, H. Mendil-Jakani, G. Gebel, J. Maier, *Phys. Chem. Chem. Phys* **2009**, *11*, 3305.
[25] K. D. Kreuer in *Handbook of Fuel Cells: Fundamentals, Technology and Applications. Volume 3: Fuel Cell Technology and Applications: Part 1*, Vol. *3* (Eds: W. Vielstich, A. Lamm, H. Gasteiger), John Wiley & Sons Ltd, Chichester, UK **2003**, pp. 420–435.
[26] W. Bras, *J. Macromol. Sci., Phys.* **1998**, *B37*, 557.